JOURNAL OF MATERIALS SCIENCE **39** (2004) 51 – 59

The role of TiO_2 and composition in the devitrification of near-stoichiometric cordierite

D. T. WEAVER, D. C. VAN AKEN, J. D. SMITH*
*Department of Metallurgical Engineering and *Ceramic Engineering, University of Missouri-Rolla, Rolla, MO 65409-0340, USA*
E-mail: dcva@umr.edu

Devitrification behavior and thermal expansion of glasses and glass-ceramics, doped with TiO_2, near the stoichiometric cordierite composition were investigated. The activation energy for growth of surface nucleated crystals was shown to be approximately 433 kJ/mol. and was independent of TiO_2 content in the glass. Volume nucleation was achieved by the addition of approximately 8 wt% TiO_2, but the mechanism of volume nucleation was different depending upon cordierite composition. Regions in the MgO-Al_2O_3-SiO_2 phase diagram near the stochiometric cordierite compound were investigated using thermal analysis, X-ray powder diffraction and dilatometry. Glass in glass phase separation was postulated for MgO-lean glasses, whereas precipitation of mullite and Al_2TiO_5 preceded devitrification in other compositions. In each case, the formation of a silica-rich glass is believed to initiate the devitrification. Coefficients of thermal expansion for the glass-ceramics increased with increasing TiO_2 content resulting from increasing levels of uncrystallized glass and the formation of mullite and rutile during crystallization.

1. Introduction

Investigators commonly refer to a wide range of magnesia-alumino-silicate compositions as cordierite even though many of these compositions, including stoichiometric cordierite ($2MgO$-$2Al_2O_3$-$5SiO_2$), are outside the cordierite primary phase field. Cordierite-based materials have drawn attention because of their low thermal expansion, low dielectric constant, and high chemical durability. Scientifically, cordierite glass-ceramics are of interest because of complexities in their devitrification, especially in the presence of various dopants and identification of the dominant crystallization mechanism, either surface or volume, has proven crucial in the manufacture of many glass-ceramic products. [1, 2].

In general, devitrification of cordierite-based glasses begins with precipitation of a metastable β-quartz, a solid-solution phase normally designated as either β-quartz$_{SS}$ or μ-cordierite. Crystallization ends with one of two polymorphs (indialite or cordierite) or a combination of the two. Although distinctions are seldom made between the two structures, since their diffraction patterns are quite similar, indialite is a disordered hexagonal phase while α-cordierite is ordered orthorhombic [3].

Although devitrification of cordierite glasses is not yet fully understood, a number of conclusions can be drawn from the literature [4–15]. Surface nucleation requires the presence of a physical alteration (abrasive scratches) and may be accelerated by either dopant additions [8] or impurities on the surface [4–6]. In cases involving the most effective nucleating agents (TiO_2, [8–13, 15] ZrO_2, [10, 12, 13, 15] and CeO_2 [13]), large dopant additions result in glass-in-glass phase separation [8–10, 12, 13] and the dopant-rich glass first yields nuclei upon which β-quartz (β-quartz$_{ss}$) grows. When doping with with TiO_2, the nucleating phase is pseudo-brookite in structure and lies between the composition limits Al_2TiO_5 and $MgTi_2O_5$ [12]. In studies by Fokin and Zanotto [8] involving nearly stoichiometric cordierite with TiO_2 additions, only the presence of Al_2TiO_5 nuclei after heat treatment was reported. Volume nucleation was most easily achieved with additions of TiO_2 in excess of approximately 8 wt% [8]. At greater concentrations of TiO_2, phase separation occurred and the pseudo-brookite phase was detected. It was also reported that surface nucleation rate increased by the addition of TiO_2 [8]. However, in Beall's work [15] with silica-rich cordierite glasses doped with TiO_2, only $MgTi_2O_5$ was found.

In a recent study [16], crystalline cordierite coatings were produced by air plasma spraying, where a minimum addition of TiO_2 was necessary to promote bulk nucleation in the coating. The purpose of the present study is to examine the role of TiO_2 in the transformation of near stoichiometric cordierite and determine the composition and structure dependence of the thermal expansion of cordierite-based glass-ceramics.

2. Experimental procedures

Scientific grade powder oxide components were batched in the approximate stoichiometric molar ratio of $2MgO\text{-}2Al_2O_3\text{-}5SiO_2$. TiO_2 was then added in a range of 0 to 10.5 wt% and the powders were thoroughly mixed. Each batch was transferred to platinum crucibles, heated to 1650°C, allowed to fine for 24 h. and cast onto a clean steel plate. The glass was subsequently crushed into pieces smaller than 2 mm, remelted in a clean platinum crucible, and cast after holding at 1650°C for 12 h.

Thermal gravitometric analysis and differential thermal analysis (TGA/DTA) was performed using a Netzch, Inc. model STA 409 to determine the crystallization behavior of each glass composition. Samples were prepared by grinding the glass in a sapphire mortar and pestle to less than 38 μm in diameter. A 240 ± 2 mg sample was weighed out of each batch, and placed in an alumina crucible. A 240 ± 2 mg powder sample (<38 μm) of pure corundum (Al_2O_3) was used as a reference. All DTA/TGA results were obtained by heating in air from 35°C to 1500°C at a rate of 10°C/min. The weight of the sample crucible and the output of both thermocouples were recorded as a function of temperature. The glass transition temperature, T_g, was determined from an inflection point while endotherm and exotherm transition temperatures were reported at the peak maximum or minimum, respectively. All transition temperatures as determined by DTA are reported to the nearest 5°C with an estimated error of ±5°C. TGA results showed no measurable weight changes over the temperature range.

Dilatometry specimens were cut to 25 ± 2 mm lengths. Glass-ceramic specimens were heated at 10°C/min. to T_g, held for 6 h, then heated at the same rate to either the first or second exotherm temperature and held for an additional 6 h. Dilation was measured at a constant heating rate of 5°C/min. from 100°C until the specimen began to deform. Additionally, other specimens were heated at 10°C/min. to T_g, held for 6 h, then heated at the same rate to 1275°C and held for an additional 20 h. These specimens transformed to the orthorhombic cordierite structure (α-cordierite) and dilation was measured from 100 to 1150°C. The thermal expansions of the materials used in this study were assumed to be linear over the temperature ranges indicated. This assumption, coupled with graphical interpretation of the dilatometry data, limits the precision of reported values to $\pm 5 \times 10^{-7}$/°C.

3. Results

Effects of TiO_2 on the devitrification behavior and thermal expansion of cordierite glasses and glass-ceramics were studied by DTA and dilatometry. Chemical analysis, DTA, and dilatometry for the same compositions are summarized in Tables I and II. DTA and dilatometry results for these compositions are plotted in Figs 1 and 2, respectively. TiO_2 additions are reported as a weight percent of the total melt. During the course of this investigation it was observed that certain composition ranges crystallized in a manner where the crystallization front was well defined and the transformation was sluggish when held at the first exotherm associated with β-quartz$_{ss}$ formation. Additional compositions were melted to investigate the composition dependence of the β-quartz$_{ss}$ transformation. All of these glasses were contained in the mullite primary phase field; however, they were separated for convenience of discussing compositional differences into regions defined by extensions of the alkemade line connecting cordierite and silica and the alkemade line connecting cordierite and mullite. The regions represent compositional ranges that result in differences in equilibrium phase assemblages as well as differences in the eutectic or peritectic melting temperatures. Although devitrification is not controlled by the prevailing equilibrium conditions, one would expect that those conditions could impact devitrification. The three regions are shown in Fig. 3 and the sluggish transformation

TABLE I DTA and chemical analysis results normalized for MgO, Al_2O_3, and SiO_2 for compositions used in dilatometry

MgO (wt%)	Al_2O_3 (wt%)	SiO_2 (wt%)	TiO_2 (wt%)	T_g (°C)	T_{quartz} (°C)	$T_{indialite}$ (°C)	$T_{cordierite}$ (°C)	T_{liquid} (°C)
13.7	32.6	53.7	0.0	835	970	1045/1070	1230	1470
13.7	35.1	51.2	2.8	820	930	1085	1265	1450
13.0	34.0	53.0	5.0	805	935	1030	1265	1430
13.1	33.6	53.3	7.8	795	925	1095	1265	1415
13.0	35.8	51.2	9.8	790	930	1140	1265	1405

TiO_2 additions are reported as a weight percent of the total melt.

TABLE II CTE and chemical analysis results normalized for MgO, Al_2O_3, and SiO_2 for compositions used in dilatometry

MgO (wt%)	Al_2O_3 (wt%)	SiO_2 (wt%)	TiO_2 (wt%)	CTE (amorphous) (10^{-7}/°C) (100–800°C)	CTE (treated at first exotherm) (10^{-7}/°C) (100–1000°C)	CTE (treated at second exotherm) (10^{-7}/°C) (100–1000°C)	CTE (treated at 1275°C) (10^{-7}/°C) (100–1150°C)	
13.7	32.6	53.7	0.0	47	21	12	24	
							(100–500°C)	(500–1150°C)
13.7	35.1	51.2	2.8	51	–	13	0	47
13.0	34.0	53.0	5.0	47	12	16	1	47
13.1	33.6	53.3	7.8	45	30	27	7	45
13.0	35.8	51.2	9.8	50	58	47	21	62

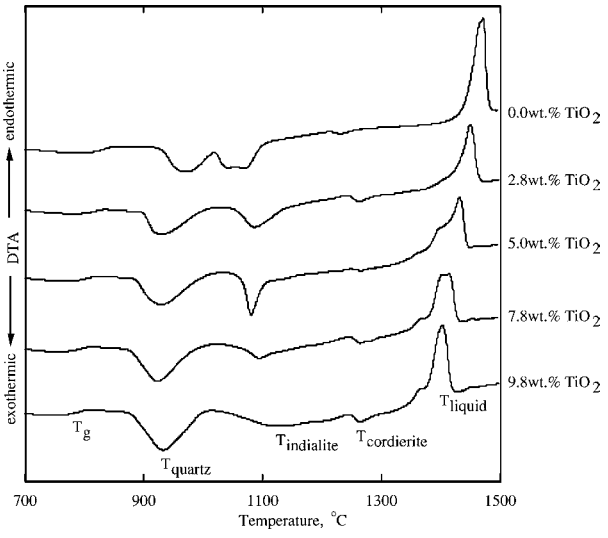

Figure 1 DTA scans of glasses used for dilatometry.

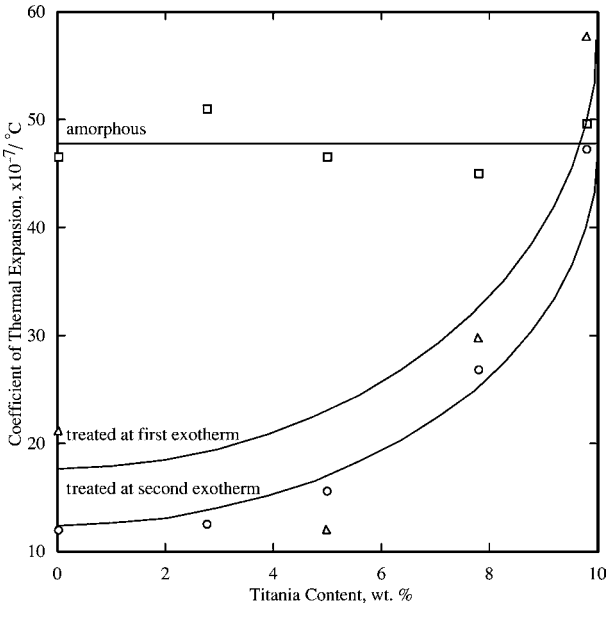

Figure 2 Graph showing the coefficient of thermal expansion of cordierite phases as a function of TiO_2 content. Lines are drawn as guides for the eye.

was observed in those compositions within region 2. Tables III through V show DTA and chemical analysis results based upon region within the mullite primary phase field.

TABLE III DTA and chemical analysis of region 1 glasses normalized for MgO, Al_2O_3, and SiO_2. TiO_2 additions are reported as a weight percent of the total melt

MgO (wt%)	14.0	13.9
Al_2O_3 (wt%)	32.4	32.7
SiO_2 (wt%)	53.6	53.4
TiO_2 (wt%)	4.9	8.3
T_g (°C)	805	790
T_{quartz} (°C)	980	955
$T_{indialite}$ (°C)	1050*	1140
T_{liquid} (°C)	1430	1410

Temperatures marked with asterisks (*) indicate estimated temperatures of peaks that appeared as shoulders of lower temperature peaks.

TABLE IV DTA and chemical analysis of region 2 glasses normalized for MgO, Al_2O_3, and SiO_2. TiO_2 additions are reported as a weight percent of the total melt

MgO (wt%)	10.9	11.2	11.7	10.9	11.1
Al_2O_3 (wt%)	33.2	36.7	30.6	34	34.6
SiO_2 (wt%)	55.9	52.1	57.7	55.1	54.3
TiO_2 (wt%)	0.0	2.9	4.5	6.5	10.4
T_g (°C)	850	835	820	810	795
T_{quartz} (°C)	1035	1005	985	970	955
$T_{indialite}$ (°C)	1075	1055*	1140	1155	1150
T_{liquid} (°C)	1470	1450	1430	1420	1395

Temperatures marked with asterisks (*) indicate estimated temperatures of peaks that appeared as shoulders of lower temperature peaks.

TABLE V DTA and chemical analysis of region 3 glasses normalized for MgO, Al_2O_3, and SiO_2. TiO_2 additions are reported as a weight percent of the total melt

MgO (wt%)	13.2	13.4	13.9	13.0	13.5
Al_2O_3 (wt%)	40.1	38.0	36.3	38.0	38.1
SiO_2 (wt%)	46.7	48.6	49.8	49.0	48.4
TiO_2 (wt%)	0.1	2.8	6.3	6.7	10.1
T_g (°C)	840	825	805	810	795
T_{quartz} (°C)	1015	985	965	965	935
$T_{indialite}$ (°C)	1090*	1070*	1030*	1105	1150
T_{liquid} (°C)	1470	1450	1430	1425	1410

Temperatures marked with asterisks (*) indicate estimated temperatures of peaks that appeared as shoulders of lower temperature peaks.

The majority of glass compositions analyzed were contained in region 2. DTA scans for glasses in region 2 are shown in Fig. 4. According to the results, increasing TiO_2 additions decreased T_g, the temperature at which the first exotherm occurs, and the first liquid formation temperature. At TiO_2 levels of 2.9 wt% and below, the weak second exotherm shifts closer in temperature to that of the first exotherm. TiO_2 additions of 4.5 wt% and greater increased the temperature difference between the first and second exotherm. This general trend is also observed in glasses in regions 1 and 3 as shown in Fig. 5. Plots of transformation temperatures as a function of TiO_2 content for glasses in regions 2 and 3 reveal that T_g, the first exotherm, and the first liquid formation temperatures decreased with increasing TiO_2 content. These plots are shown in Fig. 6.

In agreement with several other studies in the literature, the X-ray powder diffraction patterns confirm that the first exotherm is the formation of β-quartz$_{ss}$ while the second exotherm is indicative of the transformation of β-quartz$_{ss}$ to indialite. Glass-ceramics containing at least 8 wt% TiO_2 and heat treated at the first exotherm were composed predominantly of β-quartz$_{ss}$. Of the specimens heat treated at the first exotherm in each of the three regions, X-ray powder diffraction patterns exhibited trace indialite peaks for the region 3 glass containing 10.1 wt% TiO_2 only. Compositions heat treated identically and containing less than 8.3 wt% TiO_2 contained both β-quartz$_{ss}$ and indialite. Glasses containing at least 7.8 wt% TiO_2 and heat treated at the second exotherm were composed of indialite. Diffraction patterns of glass-ceramics containing less TiO_2 and heat treated identically contained trace β-quartz$_{ss}$ peaks. These results suggest that high TiO_2 additions stabilize β-quartz$_{ss}$.

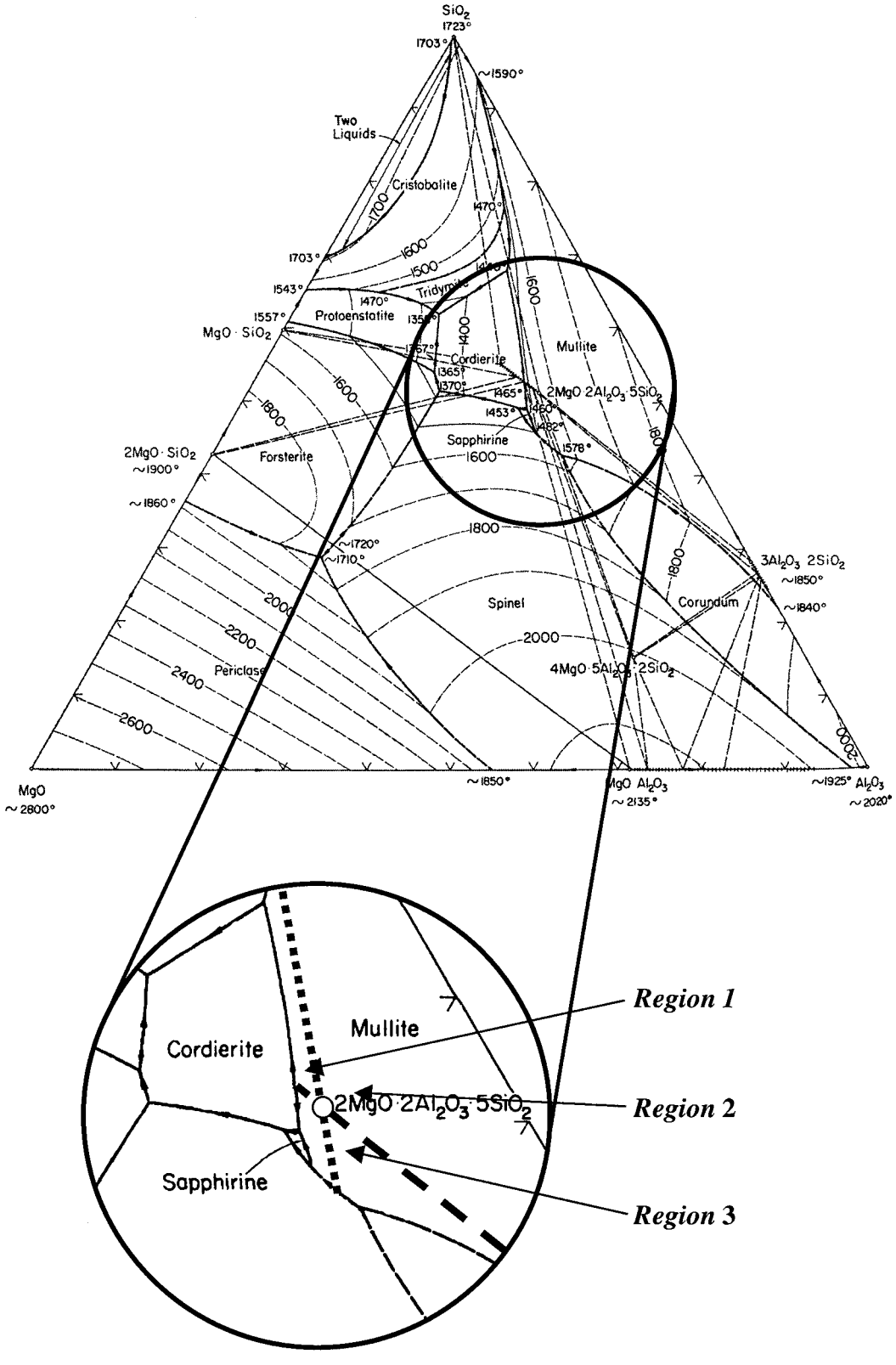

Figure 3 MgO-Al_2O_3-SiO_2 ternary diagram showing glass composition regions.

Selected diffraction scans of glasses treated at 1275°C are shown in Fig. 7. Glasses treated at 1275°C transformed to the orthorhombic cordierite crystal structure. Compositions containing less than 8.3 wt% TiO_2 contained rutile while TiO_2 additions of 8.3 wt% and greater contained both rutile and Al_2TiO_5. Additionally, compositions in region 1 containing 4.9 wt% TiO_2, region 2 containing 2.9, 4.5, 6.5, and 10.4 wt% TiO_2, and region 3 containing 2.8 and 6.7 wt% TiO_2 showed trace mullite peaks. It should be noted that the amount of mullite formed in region 2 was generally less than that observed in regions 1 or 3. Furthermore, there is little evidence of Al_2TiO_5 in the devitrified glasses from region 2. In region 3, trace anatase peaks were found in the composition containing 6.3 wt% TiO_2.

Surface crystallization with a well defined crystallization front appeared most dominant for compositions in region 2 and this presented an opportunity

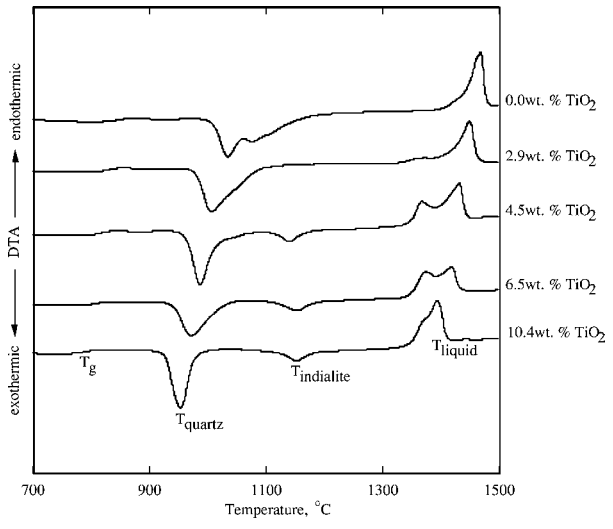

Figure 4 DTA scans of region 2 glasses.

to investigate the effects of TiO_2 on crystal growth. In order to determine the activation energy for crystal growth, glasses in region 2 containing 2.9, 4.5, and 6.5 wt% TiO_2 were treated at temperatures between T_g

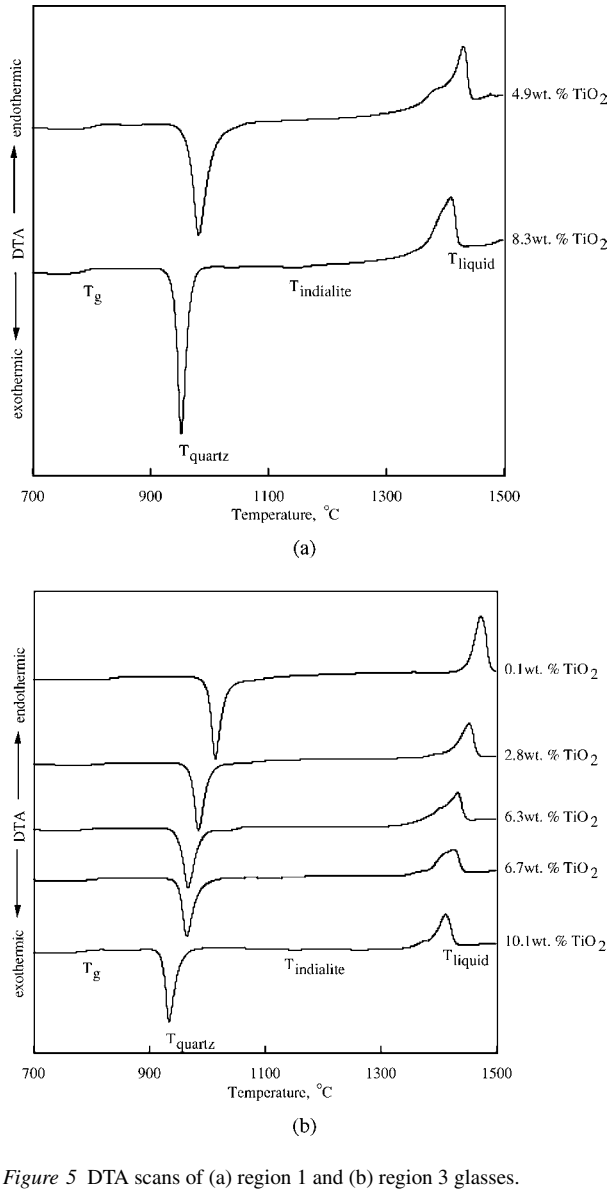

Figure 5 DTA scans of (a) region 1 and (b) region 3 glasses.

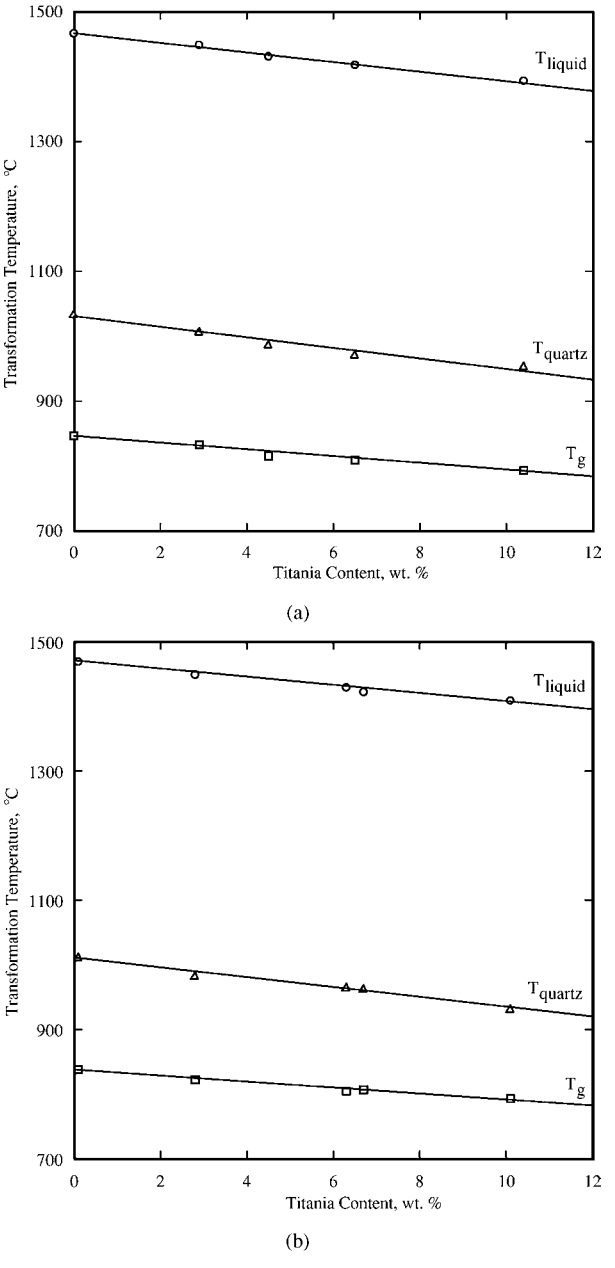

Figure 6 Glass transformation temperatures as determined by DTA as a function of TiO_2 content for glasses in (a) region 2 and (b) region 3.

and the first exotherm. Specimens were cut from the glass ribbons in lengths of approximately 10 mm. Nucleation was minimized by preheating a tube furnace to temperature prior to placing the glass specimens inside. Several specimens of each glass were transferred to the preheated furnace and systematically removed at selected time intervals. All specimens were placed onto a cordierite setter with tabular alumina between the specimens and setter to prevent reaction. Each specimen removed from the furnace was allowed to cool in still air on tabular alumina. Glass containing 2.9 wt% TiO_2 was treated at 954, 985, and 1007°C for periods up to 13.5 h. Glass containing 4.5 wt% TiO_2 was treated at 927, 956, and 984°C for a maximum of 27 h. Glass containing 6.5 wt% TiO_2 was treated at 921, 946, and 970°C for as long as 13 h. The heat treatments were ended when the specimens appeared fully crystalline.

The partially crystalline specimens were impregnated with a low viscosity resin in a vacuum oven at

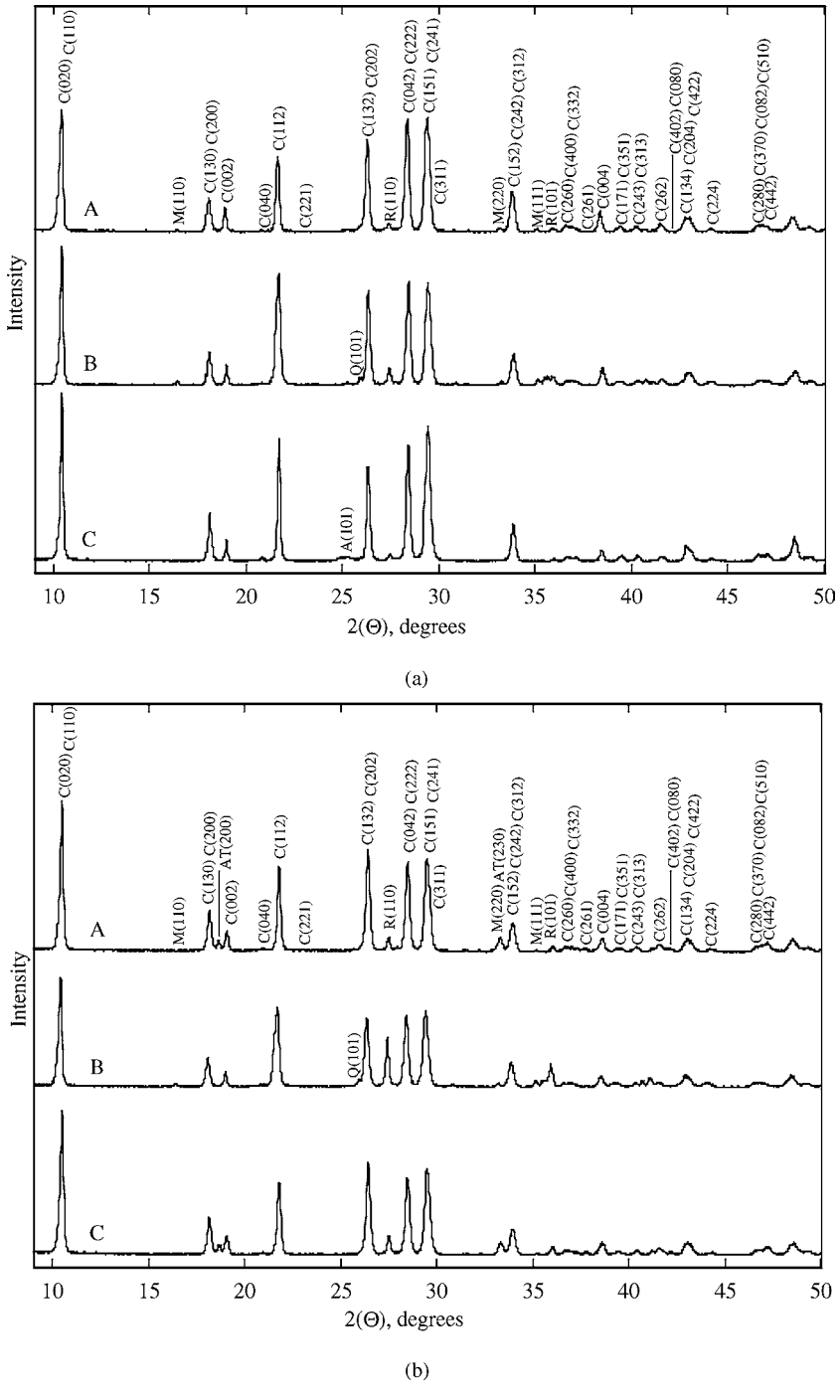

Figure 7 X-ray diffraction scans of glasses treated at 1275°C. Plot (a) shows scans for compositions (A) region 1 containing 4.9 wt% titania, (B) region 2 containing 4.5 wt% titania, and (C) region 3 containing 6.3 wt% titania. Plot (b) shows scans for (A) region 1 containing 8.3 wt% titania, (B) region 2 containing 10.4 wt% titania, and (C) region 3 containing 10.1 wt% titania. AT = Al_2TiO_5, C = orthorhombic cordierite, M = mullite, Q = β-quartz$_{ss}$, R = rutile.

60°C for 24 h to prevent spalling of the crystallized surface layer during sectioning. The impregnated specimens were sectioned with a diamond wafering blade, mounted in epoxy at room temperature, and diamond polished to 0.1 μm. Once polished, the cross sections were imaged using a cathodoluminescence (CL) microscope. Crystalline areas fluoresced a bright blue in the CL microscope while amorphous material appeared significantly darker. Measurements of the crystalline "rim" thickness were made at ten different locations on each cross section. An example CL image is shown in Fig. 8.

It has been noted previously by Diaz-Mora *et al.* [4] that surface crystals grow radially until they impinge upon one another prior to inward growth. The time required before the observance of a crystalline "rim" is manifested as an incubation time. Therefore, it can be assumed that steady state crystal growth has been achieved when the crystalline "rim" thickness becomes greater than the resolution (0.02 μm) of the CL microscope. The incubation time decreased with increasing temperature for a given glass composition, but no trend in incubation time was apparent between glass compositions.

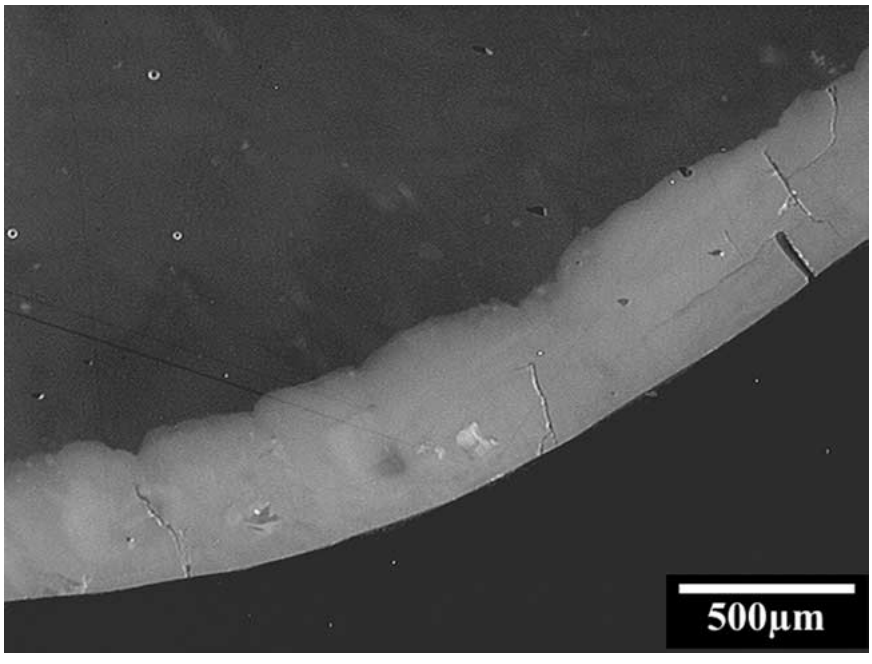

Figure 8 Cathodoluminescence image of the crystalline rim surrounding an amorphous interior of region 2 glass containing 2.9 wt% TiO_2 treated at 954°C for 48600 s.

It was assumed that the crystal growth rate was governed by an equation of the form

$$x = (k \cdot t)^{n} \tag{1}$$

where x is the "rim" thickness, k is a growth rate constant, t is the time at temperature, and n is the growth dimension exponent. The growth rate constant, k, is related to activation energy for crystal growth by

$$k = k_o \cdot \exp(-Q/RT) \tag{2}$$

where k_o is a rate constant, Q is the activation energy, R is the universal gas constant (8.314 J/mol/K), and T is absolute temperature. By taking the logarithm of Equation 1 an average growth exponent, n, was determined by regression analysis for each glass composition at the three test temperatures. An average value of n was then used for each glass to determine k by a regression analysis of x as a function of t^n. Activation energies for crystal growth in each glass were determined by plotting $\ln(k)$ as a function of the inverse absolute temperature as shown in Fig. 9. The regression of this data allowed for the determination of an average activation energy, Q, of approximately 433 kJ/mol. Results for the activation energy experiments are shown in Table VI.

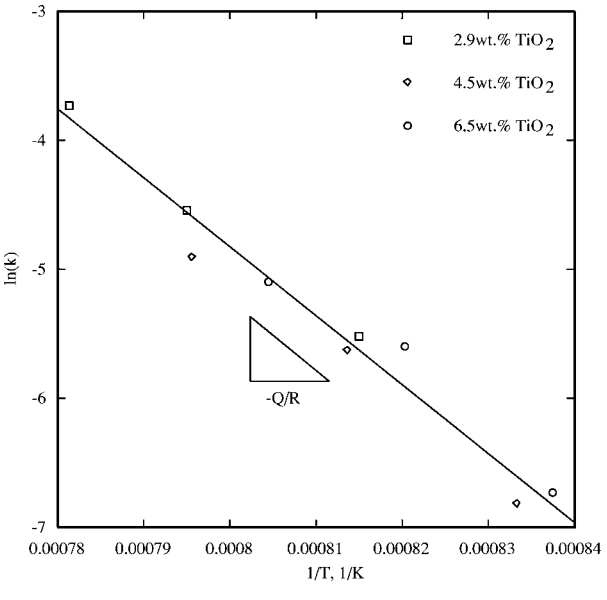

Figure 9 Plot used to determine the activation energy for inward surface crystal growth for glasses in region 2. $Q = 433$ kJ/mol. $R^2 = 0.9645$.

4. Discussion

Christian [17] recognized that the exponent, n, in Equation 1 was related to the number of dimensions in which particles grow. In the case of one and two-dimensional growth n equals 0.5 and 1, respectively. With three-dimensional growth, n is 1.5. In this study, n was determined to be 1.15 for the glass containing 2.9 wt% TiO_2, indicating two-dimensional or columnar growth and when the TiO_2 additions increased to 4.5 and 6.5 wt%, n rose to 1.41 and 1.51, respectively. These results indicate that crystallite growth behavior is dependent on the concentration of titanium cations in the glass and growth switches from two-dimensional to three-dimensional as TiO_2 additions increase.

TABLE VI Regression analyses used to determine the activation energy for crystal growth in cordierite glasses doped with TiO_2

	n^*	k (μm/s)		
2.9 wt% TiO_2	1.15	1227 K	1258 K	1280 K
		0.0040	0.0107	0.0239
4.5 wt% TiO_2	1.41	1200 K	1229 K	1257 K
		0.0011	0.0036	0.0074
6.5 wt% TiO_2	1.51	1194 K	1219 K	1243 K
		0.0012	0.0037	0.0061

The asterisk (*) indicates that an average value of n was used for each composition.

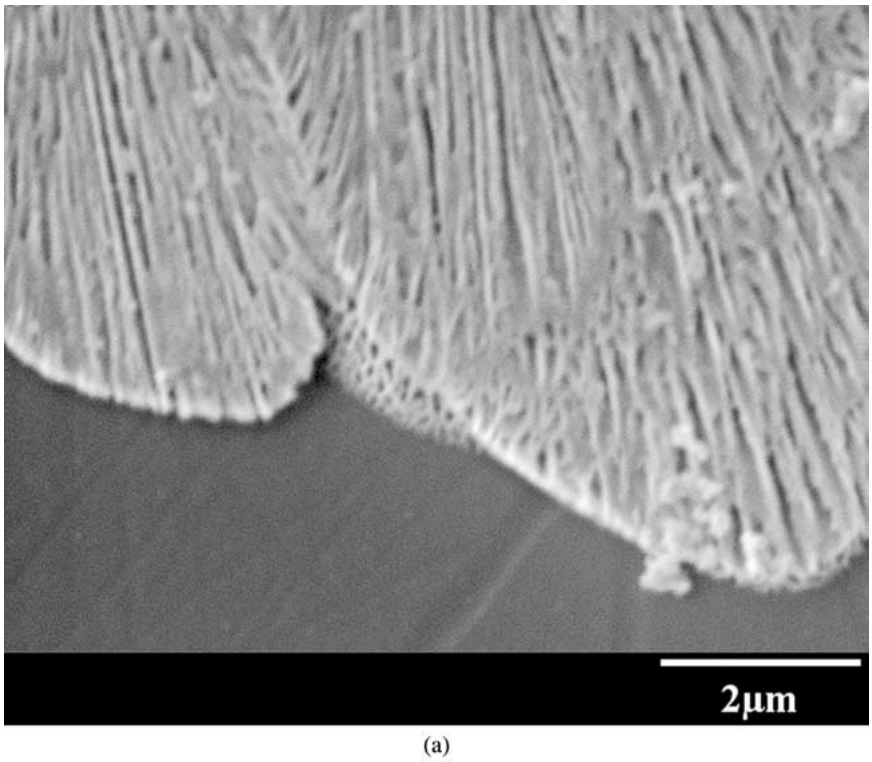

(a)

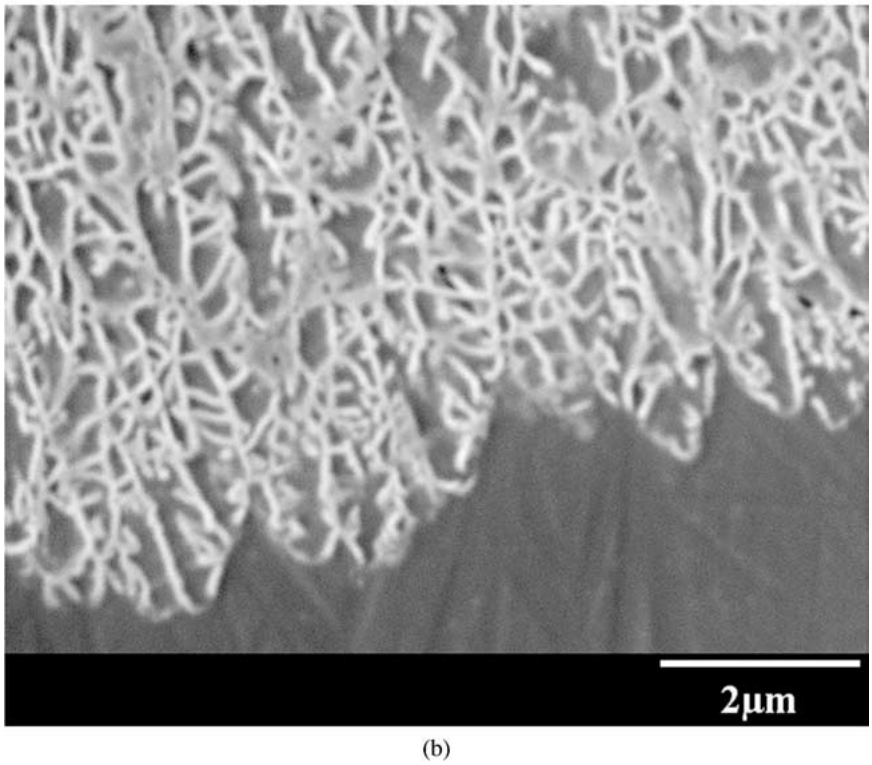

(b)

Figure 10 SEM images of partially surface crystallized cordierite glass-ceramics (a) containing 2.9 wt% TiO_2 and treated at 1007°C for 7200 s and (b) containing 4.5 wt% TiO_2 and treated at 921°C for 32400 s. Both specimens were etched with 2 vol% HF.

The theory that crystal growth switched from two-dimensional to three-dimensional between 2.9 and 4.5 wt% TiO_2 was reinforced by microscopy of partially surface crystallized specimens. As shown in Fig. 10, the inward growth of surface crystals was primarily rod-like (two-dimensional) and network-like (three-dimensional) for compositions containing 2.9 and 4.5 wt% TiO_2, respectively. Network-like growth was also observed in the glass-ceramic containing 6.5 wt% TiO_2. It is interesting to note that the change in growth morphology also corresponds to where the coefficient of thermal expansion begins to rise rapidly with increasing TiO_2 content. Thus, in addition to high expansion phases such as rutile ($90 \times 10^{-7}/°C$) and mullite ($68 \times 10^{-7}/°C$), the network structure developed with higher TiO_2 contents would contain regions of uncrystallized glass, which would also contribute to a higher thermal expansion.

The importance of the regions defined in this paper appears to be related to the formation of mullite. In regions 1 and 3, those glasses containing less than 8 wt% TiO_2 developed irregular growth fronts originating from the glass surface. We believe that the irregular growth was a result of mullite formation that preceded the β-quartz$_{ss}$ crystallization. The presence of mullite would adversely affect β-quartz$_{ss}$ growth by depleting the glass of SiO_2. In deed, Okada *et al.* [7] suggested that β-quartz$_{ss}$ becomes less stable with decreasing SiO_2 content. In region 2, less mullite forms and the crystallization can maintain a more planar front and produced a consistent rim thickness as a function of time. Furthermore, there appears to be a greater amount of rutile formed in region 2 and most likely formed later in the crystallization sequence since the β-quartz$_{ss}$ crystallization front was undisturbed. Furthermore region 2 glasses did not produce Al_2TiO_5during devitrification making rutile formation more likely.

Thermal and crystal structure analysis of the devitrified glasses in each region indicated that TiO_2 levels below 8 wt% promote the simultaneous formation of β-quartz$_{ss}$ and indialite. However, TiO_2 additions of 8 wt% and greater produced volume nucleation and reduced the amount of indialite formed with the β-quartz$_{ss}$. This has been thought to be a result of the formation of Al_2TiO_5; however, Al_2TiO_5 was not observed in region 2 glasses. We conclude that the volume nucleation of glasses in region 2 is a result of a glass in glass phase separation. Presence of Al_2TiO_5 in regions 1 and 3 cannot be separated from the mullite. It should be noted that mullite and the pseudo-brookite structure have a common interplanar spacing: (220) in mullite and (230) in Al_2TiO_5. One might argue that mullite and Al_2TiO_5 form together, which in turn nucleates β-quartz$_{ss}$ by making the glass SiO_2 rich, i.e., a SiO_2 rich glass equivalent to that formed by the glass in glass phase separation in region 2.

5. Conclusions

We conclude that the role of TiO_2 in the volume nucleated, devitrification of cordierite is to produce a SiO_2 rich glass and this is accomplished in two different manners dependent upon glass composition. The SiO_2 rich glass may result from a glass in glass phase separation in region 2 or as a result of mullite and Al_2TiO_5 precipitation in regions 1 and 3. At TiO_2 levels between 2.9 and 6.5 wt%, the activation energy for crystal growth was found to be approximately 433 kJ/mol and was independent of TiO_2 content. The mode of crystal growth was shown to be two-dimensional for glass containing 2.9 wt% TiO_2 and three-dimensional for glasses containing 4.5 and 6.5 wt% TiO_2.

Acknowledgements

The authors are grateful to Boeing Commercial Aircraft for financial support of this research. The technical monitors at Boeing were Martin A. Peterson and Dan Sanders.

References

1. J. E. SHELBY, "Introduction to Glass Science and Technology," The Royal Society of Chemistry, Cambridge, 1997.
2. C. S. RAY and D. E. DAY, *Thermochimica Acta* **280/281** (1996) 163.
3. R. CHAIM and A. H. HEUER, *J. Amer. Ceram. Soc.* **75**(6) (1992) 1512.
4. N. DIAZ-MORA, E. D. ZANOTTO, R. HERGT and R. MULLER, *J. Non-Cryst. Solids* **273**(1–3) (2000) 81.
5. N. S. YURITSIN, V. M. FOKIN, A. M. KALININA and V. N. FILIPOVICH, in "Nucleation and Crystallization in Liquids and Glasses," edited by M. C. Weinberg (AcerS, 1993) p. 379.
6. R. MULLER, D. THAMM and W. PANNHORST, in Proceedings of the 16th Int'l. Congr. Glass (1992) p. 105.
7. K. OKADA, H. KAWASHIMA, S. HAYASHI, M. SUGAI and K. J. D. MACKENZIE, *J. Mater. Res.* **13**(5) (1998) 1351.
8. V. M. FOKIN and E. D. ZANOTTO, *J. Non-Cryst. Solids* **246**(1–2) (1999) 115.
9. W. ZDANIEWSKI, *J. Mater. Sci.* **8** (1973) 192.
10. G. H. BEALL and R. C. DOMAN, in Science of Ceramics; Proceedings of the Tenth Int'l. Conf. (1980) p. 25.
11. R. C. C. MONTEIRO, M. M. R. AUGUSTO and F. FRAGATA, in Euro-Ceramics II Vol. 3: Elecroceramics and Ceramics for Spercial Applications (1991) p. 2539.
12. T. I. BARRY, J. M. COX and R. MORRELL, *J. Mater. Sci.* **13** (1978) 594.
13. W. ZDANIEWSKI, *J. Amer. Ceram. Soc.* **58**(5–6) (1975) 163.
14. J. WU and S. HWANG, *ibid.* **83**(5) (2000) 1259.
15. G. H. BEALL, in "Ceramic Technology International 1992," edited by I. Birkby (Sterling Publications Ltd., London, England, 1992) p. 89.
16. D. T. WEAVER, D. C. VANAKEN and J. D. SMITH, *Mater. Sci. Engin.* A **339** (2003) 96.
17. J. W. CHRISTIAN, "The Theory of Transformations in Metals and Alloys," Part I, 2nd ed. (Pergamon Press, New York, Inc., 1981).

Received 22 July
and accepted 14 August 2003